Relative efficiency of radiophotoluminescent glass dosimeters in a scanning pencil proton beam

Marija Majer[a*], Luka Pasariček[a], Hrvoje Brkić[b,c], Marie Davídková[d], Matěj Navrátil[e], Vladimír Vondráček[e], Željka Knežević[a]

[a] *Ruđer Bošković Institute, Zagreb, Croatia*

[b] *Faculty of Medicine in Osijek, Croatia*

[c] *Faculty of Dental Medicine and Health in Osijek, Croatia*

[d] *Radiation Dosimetry Department, Nuclear Physics Institute of the CAS, Prague, Czech Republic*

[e] *Proton Therapy Center Czech s.r.o., Prague, Czech Republic*

ABSTRACT

The increasing role of hadron therapy, and particularly of proton therapy, in cancer treatment requires dosimetric characterization of luminescent detectors in heavy charged particle beams. Ionisation density i.e. linear energy transfer (LET) is changing when heavy charged particle is penetrating through a material. Therefore, it is crucial to evaluate how efficiency of the used dosimeters depends on the change in LET.

The aim of this study was to evaluate relative efficiency of RPL glass dosimeters type GD-352M as a function of LET in a clinical scanning pencil proton beam of 100 MeV and compare it to the results obtained with thermoluminescent (TL) dosimeters type TLD-100. LET_f and LET_d at the selected dosimeter's position were evaluated and compared by two Monte Carlo codes (MCNP and PHITS). Linear dose response is precondition for the evaluation of dosimeter efficiency and first, dose response in proton beam was evaluated and compared with those in ^{60}Co gamma ray field.

Linear dose response up to 9 Gy was confirmed for RPLs in proton beam, and gamma ray field. For TLDs, supralinearity from about 5 Gy was observed. A constant relative efficiency is observed along the plateau (corresponding to LET_f from 0.7 keV/μm to 1.7 keV/μm) of non-modulated proton beam with an average value 1.00 ± 0.02 for RPL and 0.97 ± 0.02 for TL dosimeters. Relative efficiency decrease of 10% is observed for RPLs within the Bragg peak with LET_f = 2.3 keV/μm. Future work will be focused on the evaluation of the efficiency for higher LET values using more energetic proton beams and precise positioning along the Bragg peak.

Keywords: dose response, relative efficiency, RPL glass dosimeter, TLD-100, proton therapy

1. Introduction

Luminescent detectors are widely applied in clinical dosimetry, particularly for different dosimetry measurements in gamma fields. Due to low sensitivity to neutrons, radiophotoluminescent (RPL) detectors are also convenient to use for gamma dosimetry in mixed gamma + neutron fields (Miljanić et al., 2008; Stolarczyk et al., 2018) while combination of different thermoluminescent (TL) lithium fluoride detectors (with different sensitivity to neutrons depending on the lithium isotope abundance) can be used to obtain information about neutron dose (Stolarczyk et al., 2018). The increasing role of hadron therapy in cancer treatment requires dosimetric characterization of luminescent detectors in heavy charged particle beams. Ionisation density i.e. linear energy transfer (LET) is changing when heavy charged particle is penetrating through a material. Therefore, it is very important to evaluate how efficiency of a detector depends on the change in LET. Although different TL and optically stimulated luminescent (OSL) detectors have been investigated in heavy charged particle beams in many studies (Bilski, 2011; Sadel et al., 2014; Sadel et al., 2016; Yukihara et al., 2015), there are not many studies for RPL detectors. Particularly, studies related to the relative efficiency are rare. On the other hand, very useful advantage of RPL detectors over other luminescent detectors is possibility of multiple readout and new studies in proton and heavier charged particle beams are greatly encouraged.

The most known and widely used RPL material is silver activated phosphate glass (Yamamoto, 2011) and it was of concern in this study. Recent development of other RPL materials and the prospects are given in a recent review by Yanagida et al (2022). The linear dose response of silver activated phosphate glass detectors, as an important precondition to use them as dosimeters, was reported in the previous studies by measuring the RPL signals for doses up to 500 Gy in gamma ray fields (Kodaira et al., 2018, Son et al, 2011, Hsu et al, 2011; Rah et al., 2009, Araki et al, 2014). On the other hand, only two studies devoted to heavy charged particle beams were found. For clinical proton beam, Rah et al. (2012) have used RPL dosimeters type GD-301 which are commonly used for clinical dosimetry and reported linear dose response up to 10 Gy. Majer et al. (2023) investigated dose response of RPL glass detectors using low energy (stopping) proton, lithium and carbon ion beams and reported linearity for doses higher than 10 Gy.

For linear dose response range, it is essential to determine luminescence efficiency as a function of LET before usage of dosimeters in ion fields. Unlike other luminescent dosimeters, there are not many studies related to the efficiency of RPL dosimeters. In two studies (Yasuda and Fujitaka, 2000; Kodaira et al., 2018) RPL glass detectors, taken from environmental and personal dosimeters, were exposed to different high energy ion beams and a constant efficiency for LET in water (LET_w) of less than 0.5 keV/μm and 2 keV/μm were reported and decrease of efficiency when LET_w exceeds these values. Majer et al. (2023) reported decreased relative efficiency of RPL glass detectors exposed to low energy proton, lithium and carbon beams with LET_w values higher than 8.1 keV/μm. Relative efficiency for RPL dosimeters type GD-302M using clinical, high energy, scattered and scanned pencil proton beams with LET_w values up to 10 keV/μm was investigated in several studies (Chang et al., 2017, Yasui et al., 2021, Nagata et al, 2021) and decrease of efficiency with increase of LET_w was reported.

The aim of this study was to investigate following dosimetric characteristics of RPL glass dosimeters type GD-302M: 1. dose response obtained in clinical active scanning proton beam of 100 MeV and reference ^{60}Co gamma ray field and 2. relative efficiency as a function of LET values along the Bragg curve. The results were compared with those obtained with TL dosimeters type TLD-100. Additionally, for the calculation of LET values in water (fluence and dose averaged, LET_f and LET_d) at the dosimeter's position along the Bragg curve, two Monte Carlo (MC) codes (PHITS and MCNP) were used and compared.

2. Materials and methods

2.1. Dosimetry systems

In present study RPL and TL dosimetry systems were used. Calibration for both types of dosimeters was obtained in the reference, ^{60}Co gamma ray field in the Secondary Standard Dosimetry

Laboratory (SSDL) at the Ruđer Bošković Institute (RBI) (Vekić et al., 2006). The detailed procedures of dose calculations, characteristics and principles of RPL and TL dosimetry systems are given in previously published papers (Knežević et al., 2011; Knežević et al., 2013; Miljanić et al., 2002).

The RPL dosimeters type GD-302M are silver activated phosphate glass rods with 1.5 mm in diameter and 12 mm length packed in a plastic holder (outer dimensions: Φ 4.3 mm × 14.5 mm) (ATGC, 2007). Effective atomic number and density of the glass dosimeters are 12.039 and 2.61 g/cm^3, respectively. Dose Ace FGD-1000 automatic reader equipped with a pulsed ultraviolet laser was used for the readout of the dosimeters. Prior to irradiations the RPL dosimeters were annealed at 400°C for 20 min and after irradiation, before readout, in order to build up the signal the dosimeters were preheated at 70°C for 30 min. There was no need for individual sensitivity correction factors (Knežević et al., 2011).

The TL dosimeters were ^{nat}LiF:Mg,Ti (type TLD-100) produced by Thermo Fisher Scientific in the form of small cylindrical pellets with 4.5 mm diameter and 0.9 mm height and with effective atomic number of 8.3. The dosimeters were readout using Toledo 654 Vinten reader with maximum readout temperature of 270°C and heating rate of 10°C/s. Prior to irradiation the dosimeters were annealed at 400°C for 1 hour following by 2 hours at 100°C and before the readout the dosimeters were preheated 100°C for 20 min. Before the measurements individual sensitivity correction factors were determined for the used TLDs. The dosimeters were irradiated to a uniform dose of 5 mGy (kerma „free in air") using the ^{137}Cs source in the SSDL at the RBI (Vekić et al., 2006).

2.2. Experimental set-up

2.2.1. Irradiations with the clinical proton beams

Irradiations using scanning proton pencil beams were carried out at the Proton Therapy Center (PTC) Czech s.r.o. in Praque. 100 MeV beams accelerated in the isochronous Proteus C-235 cyclotron from Ion Beam Application were delivered to the radiotherapy treatment room equipped with gantry and used for irradiation of dosimeters. For all irradiations single energy beams were used and the field dimension were (20 × 20) cm^2. All measurements were performed in SSD geometry (gantry angle 0°

and isocentre was placed on the surface of the measurement phantom). Reference proton beam dosimetry was performed with the Plane Parallel Chamber PPC05 positioned in the central part of the field. Treatment Planning System (TPS) RayStation (RaySearch Laboraties) was used for the field preparation and calculation of the 3D dose distribution in water.

Dosimeters were placed in a polymethylmethacrylate (PMMA) holders with dimensions $(8 \times 8 \times 0.5)$ cm^3. The holders were prepared to accommodate five TL and three RPL dosimeters as shown in Fig. 1. (a). For every irradiation, the average value for five or three dosimeters and standard deviation of the mean were calculated and used for the further calculations. For comparison, at the same time, measurements with PPC05 were performed as shown in Fig. 1. (b). All results were expressed as dose to water, D_w.

To determine dose response function, the holders with dosimeters were placed on the patient treatment couch and irradiated in the dose range from 0.5 Gy to 9 Gy from the top.

To measure dose-depth distribution, the position of dosimeters along the Bragg curve was adjusted using RW3 slabs with dimensions (30×30) cm^2 placed on the holder (Fig. 1. (b)). To avoid instability of the experimental setup, additional PMMA holders were placed around the holder with dosimeters. The entrance dose for the measurement set-up without any RW3 plate was 1 Gy. By adding RW3 slabs (total thickness was 1, 2, 3, 4, 4.5, 5, 5.5, 6, 6.5, 7 cm), measurements were made at different depths along the Bragg curve. To evaluate the depth at which dosimeters were positioned, the water equivalent thickness (WET) of the RW3 slabs was taken into account (1.026 cm). Material behind the dosimeters was not considered because of low contribution of backscattered protons (less than 0.1%).

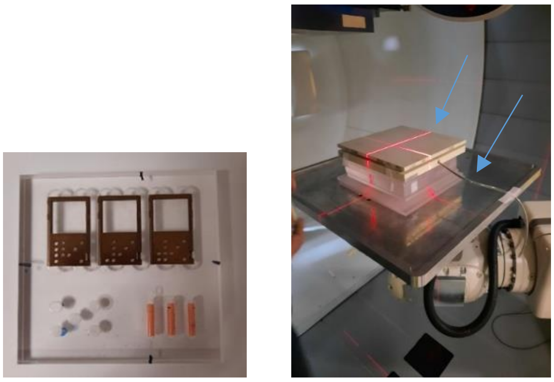

a) b)

Fig. 1. PMMA holder with dosimeters (a) and experimental setup (b). For measurements of the dose-depth distribution RW3 slabs are placed on the holder.

2.2.2 Irradiations in the ^{60}Co gamma ray field

Gamma irradiations were performed in the SSDL at the RBI using ^{60}Co gamma ray source (Vekić et al., 2006). For all purposes, dosimeters were irradiated in terms of air kerma free in air (uncertainty 1.2% (k = 2)). K_{air} values were measured with the reference ionization chamber (IC) and conversion to dose to water, D_w, was made with conversion factor of D_w/K_{air} = 1.112 (NIST, 2008).

To check dose linearity, dosimeters were irradiated to the following doses (K_{air} = 0.1, 0.5, 1, 2, 3.2, 4.5, 5 and 8.5 Gy). For each dose, five TLDs and three RPLs were irradiated and the average value and standard deviation of the mean for each type of dosimeters were calculated. For the calculation of the relative efficiency, K_{air} = 0.5 Gy irradiation was used as the reference irradiation. For calibration, calibration dosimeters were exposed to K_{air} = 0.5 Gy.

2.3. Evaluation of dosimetric quantities

The linearity index, *f(D)*, is determined according to the following formula (Olko and Bilski, 2020):

$$f(D) = \frac{I(D)/D}{I(D_0)/D_0} \quad (1)$$

where *I(D)* is the TL or RPL signal obtained at a dose *D* and $I(D_0)$ is the TL or RPL signal obtained at a reference dose D_0 where the dose response of luminescent dosimeters is linear. In the present study, dose level used for calibration of dosimeters (K_{air} = 0.5 Gy) is used for D_0 and linearity index is determined for 100 MeV proton beam and ^{60}Co gamma ray irradiations. Dose values, D and D_0, are measured by the reference dosimeter (PPC05 for proton irradiations and IC for gamma ray irradiations).

The relative efficiency of luminescent dosimeters indicates the amount of luminescence light emitted for a given type of radiation with respect to the light emitted for a reference radiation (typically ^{137}Cs or ^{60}Co gamma rays). The TL and RPL efficiency for protons with different energies (*i.e.* LET values) relative to the reference gamma rays, $\eta_{p,\gamma}$(LET), is determined using equation (Bilski et al, 1994; Olko and Bilski 2020):

$$\eta_{p,\gamma}(LET) = \frac{[I_{LET}(D)/D]_p}{[I(D)/D]_\gamma} \quad (2)$$

where the numerator represents the TL or RPL signal, $I_{LET}(D)$, per unit dose, D, measured by the reference dosimeter for proton irradiation and the denominator represents the same for the reference (K_{air} = 0.5 Gy) ^{60}Co gamma ray irradiation. Dose levels, D_p and D_γ, must be in the linear dose response region (Horowitz et al., 2006) and therefore dose linearity check is the precondition for determination of the relative efficiency. In the following sections, relative efficiencies for RPL and TL dosimeters calculated by eq. (2) are referred as η_{RPL} and η_{TLD}.

2.4. Monte Carlo simulation

To determine relative efficiency for the selected detectors as a function of varying LET, LET values at the detector position were obtained using MC simulation. The fluence averaged LET (LET_f) and the dose averaged LET (LET_d) (Kalholm et al., 2021) in water were calculated using Monte Carlo N-Particle transport code 6.2 (MCNP) (Werner et al., 2018) and PHITS (version 3.31) (Sato et al., 2018). Cross-section data used in the simulation for both codes and chemical composition of all the materials are given in Table 1.

Table 1

The density, elemental composition and cross-section data for the materials used in the MC simulations. The elemental composition is given in terms of nuclides and their respective relative weights. The cross section dana listed for PHITS for neutrons was used up to 20 MeV.

Material	Elemental composition (relative weight)	Density [g/cm^3]	Cross-sections				
				PHITS(3)		MCNP(3)	
Dry Air	N-14 (0.75527)	0.001205	H	1001	50c	1001	80c
	Ar-40 (0.01282)			1000	50p		70h
	O-16 (0.23178)		C	6012	50c	6012	80c
	C-12 (0.00012)			6000	50p		70h
RW3(1)	C-12 (0.9041)	1.045	N	7014	50c	7014	80c
	H-1 (0.0759)			7000	50p		70h
	Ti-22 (0.012)		O	8016	50c	8016	80c
	O-16 (0.008)			8000	50p		70h
Water	O-16 (0.888106)	0.998	Ar	7014	50c	18040	80c
	H-1 (0.111894)			7000	50p		70h
			Ti	18040	62c	22000	62c
					model(2)		model

(1) Asgari et al. (2015)
(2) Boudard et al. (2013), Hirayama et al. (2005), Iida et al. (2007)
(3) c denotes continuous-energy neutron data libraries, h proton data libraries and p denotes photon data libraries

A total number of $2 \cdot 10^8$ initial proton particles were transported for the calculation using MCNP with a resulting statistical uncertainty below 0.1%. F6 tally was used for recording the dose and for the LET calculation F4 tally with LET special treatment were used.

PHITS simulations were performed with 10^9 initial proton particles (maxbch × maxcas = $10^6 \times 10^3$) and resulting statistical uncertainty was below 0.1%. The deviations from the default settings were the use of energy (nedisp = 1) and angular (nspred = 2) straggling for protons. In addition, electrons, positrons and photons were transported using the EGS5 algorithm (negs = 1), and Event Generator mode Version 2.1 (e-mode = 2) was used. The absorbed dose was tallied using [T-Deposit], while the LET spectra were scored using [T-LET].

The beam size was (20 × 20) cm^2 and the source input was derived from the comparison of the normalized simulated depth dose distribution in water with that given by TPS. For that purpose, both MC codes scored absorbed dose within xyz grid (2 × 2 × 0.025) cm^3 along the beam direction (positive z axis). The best agreement with values given by TPS was obtained using (101.3 MeV, FWHM = 2.0%) beam by PHITS and (101.2 MeV, FWHM = 1.9%) beam by MCNP. Comparison was performed for the parameters: peak to plateau ratio defined as the ratio of the Bragg peak (BP) dose to the entrance dose, R90 value defined as the interpolated value from the depth-dose distribution with the 90% dose in the distal falloff and, full width at half maximum (FWHM). Comparison of the parameters obtained by MC codes and TPS is shown in Table 2.

Table 2

Comparison of the non-modulated Bragg curve parameters calculated with MC simulations and TPS.

	BP to plateau ratio	R90 [mm]	FWHM [mm]	Modulation width [mm]
TPS	4.35	77.9	10.1	2.11
PHITS	4.80	77.9	9.9	2.18
MCNP	4.32	77.9	11.1	2.25

Geometry of the experimental set-up with RW3 slabs was modelled with both MC codes to match irradiation conditions described in the section 2.2.1. The primary proton LET spectra were tallied for both MC codes at the location of detector position within rectangular water cell with dimension 1 cm × 1 cm (perpendicular to the beam) × 0.1 cm (along the beam direction), while binning was done in logarithmic scale ranging from 0.1 to 20 keV/µm in 200 bins.

2.5. Uncertainties

The combined uncertainties for *f(D)* and $\eta_{p,\gamma}$(LET) are estimated following the guidelines (JCGM, 2008) and expressed with a coverage factor k = 1. Uncertainty components are related to the determination of the RPL or TL signal, *I(D)*, and to the absorbed dose measured by the reference dosimeters (the type B component obtained from the SSDL and PTC). A standard uncertainty of *I(D)* is calculated as the standard deviation of the mean reading for three RPL and five TL dosimeters irradiated under the same conditions.

3. Results

3.1 Dose response

Fig. 1 shows the dose response of RPL and TL dosimeters for ^{60}Co gamma ray and 100 MeV scanned pencil proton beam irradiation. Reference doses were measured using IC and PPC05. Linear fitting procedure has been applied and equations obtained together with R^2 values are shown in Fig. 1. Results for TLDs obtained for the reference dose higher than 5 Gy are not included in the linear fitting because the *f* values were 1.08 and 1.14. Comparison of measured doses with uncertainties for proton and gamma irradiation is shown in Table 3 and Table 4, respectively. Linearity index, *f*, is given also in Table 3 and Table 4.

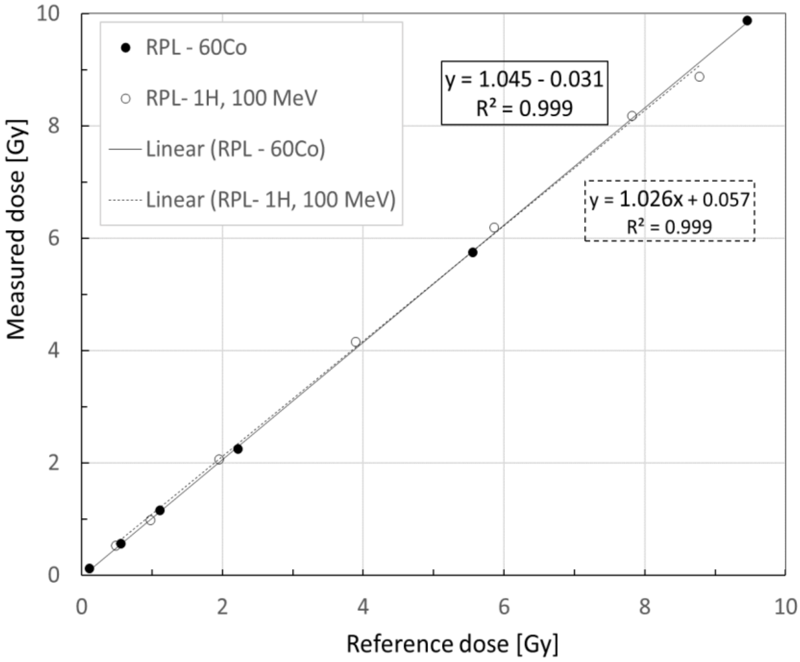

a)

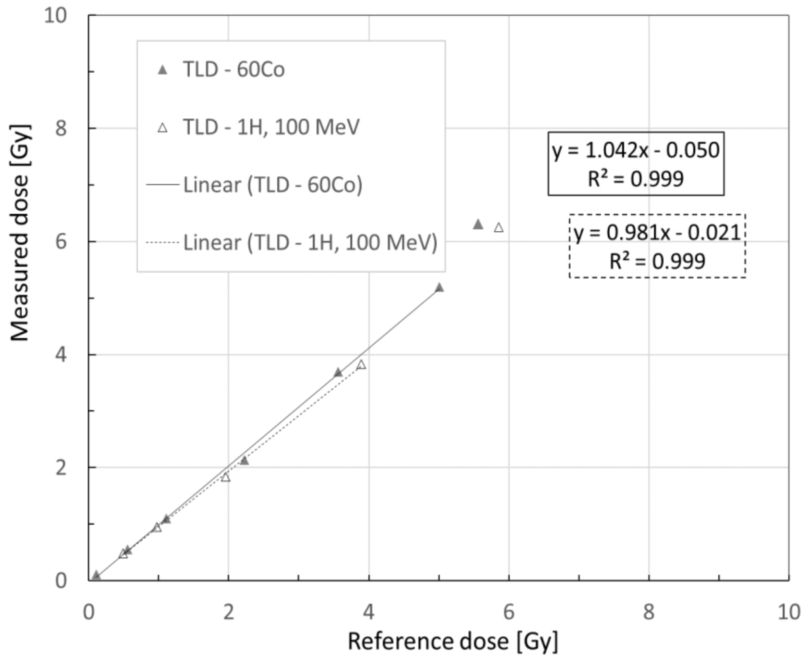

b)

Fig. 1. Dose response for RPL glass dosimeters (GD-302M) (a) and TL dosimeters (TLD-100) (b) in ^{60}Co gamma ray and 100 MeV proton beam irradiations. Equations and R^2 values for linear fits are shown. Uncertainties are given in Table 3 and Table 4.

Table 3

Linearity index, *f*, and doses measured with PPC, TL and RPL dosimeteres in 100 MeV scanning pencil proton beam. Standard deviations of the mean values for RPL and TL dosimeters are also given. Relative difference Δ is defined as $(D_{w,PPC} - D_{w,lum.dosimeter})/D_{w,PPC}$.

$D_{w,PPC}$ [Gy]	$D_{w,TLD}$ [Gy]	$D_{w,RPL}$ [Gy]	$\Delta_{PPC,TLD}$ [%]	$\Delta_{PPC,RPL}$ [%]	f_{TLD}	f_{RPL}
0.489	0.484 ± 0.002	0.525 ± 0.004	1.0	–7.4	1.00	1.00
0.975	0.946 ± 0.003	0.981 ± 0.001	3.0	–0.6	0.98	0.94
1.953	1.833 ± 0.004	2.060 ± 0.008	6.1	–5.5	0.95	0.98
3.896	3.8 ± 0.5	4.15 ± 0.03	1.8	–6.5	0.99	0.99
5.859	6.3 ± 0.1	6.19 ± 0.06	–6.8	–5.5	1.08	0.98
7.823	-	8.18 ± 0.01	-	–4.6	-	0.97
8.778	-	8.9 ± 0.1	-	–1.1	-	0.94

Table 4

Linearity index, *f*, and doses measured with IC, TL and RPL dosimeters in ^{60}Co gamma ray field. Standard deviations of the mean values for RPL and TL dosimeters are also given. Relative difference, Δ, is defined as $(D_{w,IC} - D_{w,lum.dosimeter})/D_{w,IC}$.

$D_{w,IC}$ [Gy]	$D_{w,TLD}$ [Gy]	$D_{w,RPL}$ [Gy]	$\Delta_{IC,TLD}$ [%]	$\Delta_{IC,RPL}$ [%]	f_{TLD}	f_{RPL}
0.111	0.113 ± 0.001	0.114 ± 0.004	−1.4	−2.4	1.01	1.02
0.556	0.556 ± 0.007	0.56 ± 0.01	0.2	0.1	1.00	1.00
1.112	1.11 ± 0.01	1.15 ± 0.02	0.7	−3.6	0.99	1.04
2.224	2.13 ± 0.03	2.24 ± 0.03	4.2	−0.9	0.96	1.01
3.558	3.69 ± 0.06	-	3.7	-	1.04	-
5.004	5.20 ± 0.03	-	−3.9	-	1.04	-
5.560	6.32 ± 0.07	5.74 ± 0.08	−13.6	−3.2	1.14	1.03
9.452	-	9.9 ± 0.3	-	−4.5	-	1.04

3.2. Relative efficiency

Absorbed doses measured with RPL, TL and PPC05 dosimeters along the Bragg curve in the RW3 phantom and relative RPL and TL efficiencies are shown in Fig. 2. (a). The relative efficiencies are calculated using eq. (2) and in the following text referred as η_{RPL} and $\eta_{TLD.}$ Depth in RW3 is expressed as d_{WET}. Relative efficiencies and LET values at the dosimeter's position are given in Table 5. LET_d and LET_f were calculated using PHITS and MCNP codes. To enable comparison with other studies, the LET_w for a given position of dosimeter was calculated using SRIM code (Ziegler et al., 2010) and given also in Table 5. Fig. 2. (b) shows different LET quantities, calculated for water, as a function of depth for the non-modulated proton beam used in the study.

In the following sections, plateau refers to LET_f range (0.7 - 1.7) keV/μm, that corresponds to proton energy range (100 - 35) MeV and Bragg peak (BP) refers to higher LET (i.e. lower energy) values.

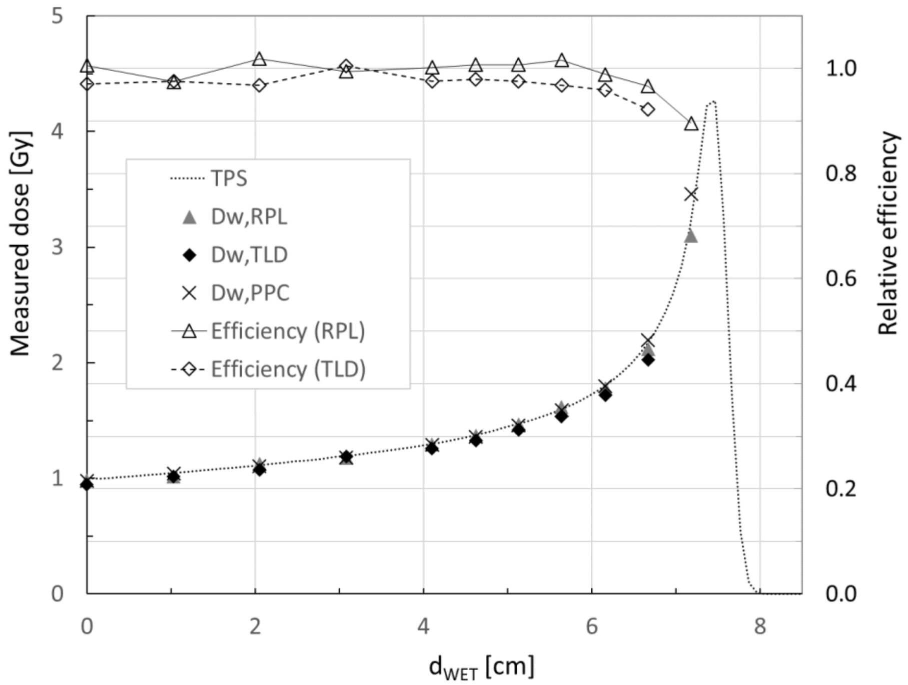

a)

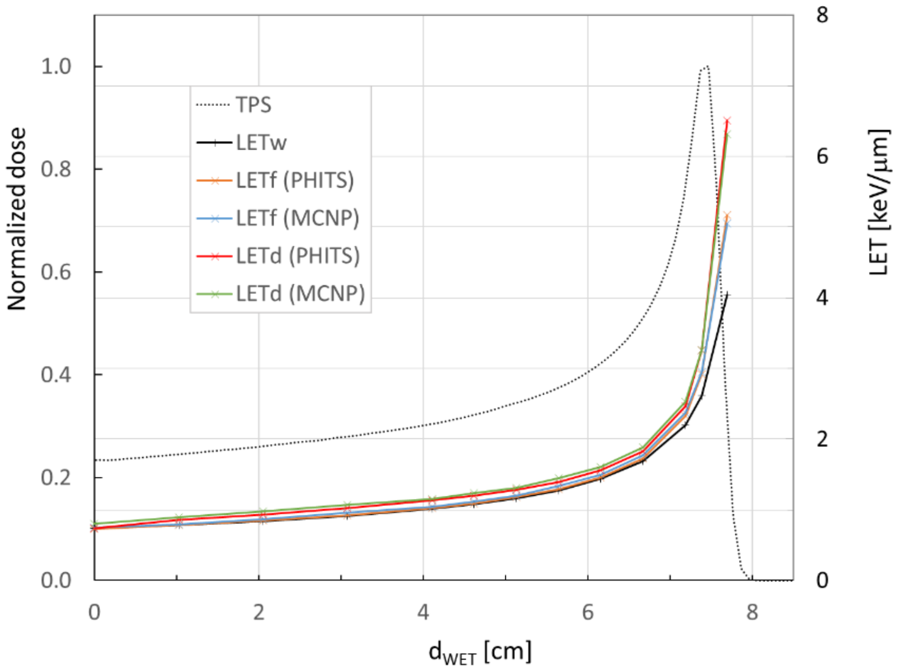

b)

Fig. 2. (a) Doses measured with RPL and TL dosimeters (full symbols) and reference dose measured with PPC05. TPS values are shown with dotted line. Relative efficiency for both luminescent dosimeters is shown with open symbols. Uncertainties are given in Table 5 (b) Calculated LET values as a function of $d_{WET.}$

Table 5

Relative efficiency, η, for RPL and TL dosimeters. For each dosimeter's position, WET depth and calculated LET_f , LET_d and LET_w are given.

d_{WET} [cm]	LET_w (SRIM) [keV/μm]	LET_f (PHITS) [keV/μm]	LET_d (PHITS) [keV/μm]	LET_f (MCNP) [keV/μm]	LET_d (MCNP) [keV/μm]	η_{RPLD}	η_{TLD}
0.000	0.74	0.73	0.74	0.75	0.81	1.01 ± 0.01	0.97 ± 0.01
1.026	0.78	0.78	0.86	0.80	0.90	0.97 ± 0.01	0.97 ± 0.01
2.052	0.84	0.85	0.94	0.87	0.98	1.02 ± 0.01	0.97 ± 0.01
3.078	0.91	0.92	1.02	0.96	1.07	0.99 ± 0.01	1.01 ± 0.02
4.104	1.01	1.03	1.13	1.04	1.16	1.00 ± 0.01	0.98 ± 0.01
4.617	1.08	1.09	1.20	1.12	1.23	1.01 ± 0.03	0.98 ± 0.01
5.130	1.16	1.18	1.28	1.20	1.32	1.01 ± 0.04	0.98 ± 0.01
5.643	1.28	1.29	1.39	1.34	1.45	1.02 ± 0.03	0.97± 0.01
6.156	1.44	1.46	1.56	1.50	1.60	0.99 ± 0.01	0.96 ± 0.01
6.669	1.69	1.73	1.83	1.77	1.88	0.97 ± 0.01	0.92 ± 0.01
7.182	2.20	2.32	2.47	2.37	2.53	0.90 ± 0.01	-

4. Discussions

4.1 Dose response

Results for R^2 and f obtained in this study indicate linear dose response of RPL dosimeters type GD-302M up to 9 Gy for ^{60}Co gamma rays and 100 MeV scanning pencil proton beam. The previous studies, which reported linear dose response by measuring the RPL signal at the dose level > 0.5 Gy, are listed in Table 6. Majority of studies are related to the gamma ray fields and just one (Rah et al, 2012) is related to the clinical, passive scattered proton beam and reported linearity for the same dose range as in this study. Rah et al. (2012) used RPL dosimeter type GD-301 and reported, based on R^2 value of 0.998, linear dose response up to 10 Gy for TLD-100, as well. As in this study, higher linearity slope for RPL dosimeters in comparison to TLD-100 is observed by Rah et al. (2012).

In the case of thermoluminescent LiF:Mg,Ti dosimeters (such as TLD-100), supralinear dose response is reported in many studies. In general, a few Gy is reported to be a threshold for the supralinearity for the main dosimetric peak, but exact value varies across the studies and type of dosimeters (Olko et al, 2001, Bilski et al, 2004, Avila et al, 2006, Massilon-JL et al, 2006). Results obtained in this study ($R^2 > 0.999$ and $f < 1.04$) suggest linearity up to 3.9 Gy and supralinearity from 5.9 Gy for 100 MeV proton beam, and linearity up to 5.0 Gy and supralinearity from 5.6 Gy for the gamma rays. It should be noted that if all results (including points with $f = 1.08$ and 1.14) are included in the linear fitting procedure, R^2 values obtained decreases to 0.996 and 0.994 which may be still recognized as linearity. Therefore, both linear fitting and linearity index are necessary to properly evaluate the results.

Table 6

Studies reported linear dose respons of RPL glass dosimeters at dose level > 0.5 Gy.

Reference	Radiation	Dose range	Dosimeter
Kodaira et al., 2018	^{137}Cs	30 μGy – 10 Gy	RPL glass
Rah et al., 2009	^{60}Co	0.5 Gy – 3 Gy	GD-301
Kato et al., 2014	$80kV_p$	0.1 Gy – 3 Gy	GD-302M
Weselowska et al., 2017	^{60}Co	1 Gy – 4 Gy	GD-302M
Oonsiri et al., 2019	6MV	0.01 Gy – 3 Gy	GD-302M
Son et al., 2011	^{60}Co	1 Gy – 500 Gy	GD-302M
Araki et al., 2004	6MV	0.5 Gy – 30 Gy	GD-301
Hsu et al., 2007	^{60}Co	0.01 Gy – 100 Gy	GD-302M
Hsu et al., 2011	^{60}Co	3 Gy – 120 Gy	GD-302M
Rah et al., 2012	Clinical 230 MeV ^{1}H	1 Gy – 10 Gy	GD-301
Majer et al., 2023	(1 – 5) MeV ^{1}H 12 MeV ^{7}Li 15 MeV ^{12}C	5 Gy – 115 Gy[(1)] 120 Gy – 620 Gy[(1)] 315 – 2500 Gy[(1)]	RPL glass
This study	^{60}Co Clinical 100 MeV ^{1}H	0.1 Gy – 9.5 Gy 0.5 Gy – 8.8 Gy	GD-302M

[(1)] dose to RPL glass

4.2 Relative efficiency

The relative luminescence efficiency as a function of LET is important precondition for the use of dosimeters in the densely ionising radiation such as protons and heavier charged particles. It is also important to specify which LET quantity and which method was used to determine LET. In the present study, LET_f and LET_d values were calculated using two MC codes (PHITS and MCNP) as it is often case in the majority of nowadays studies. The relative difference for the same LET quantity obtained with PHITS and MCNP was below 5%. As shown in Fig 2.b and Table 5, the LET_f values in the plateau ranged from 0.7 keV/μm (corresponding to proton energy of 100 MeV) for d_{WET} = 0 cm to 1.7 keV/μm (corresponding to 34.8 MeV) for d_{WET} = 6.7 cm. BP is characterized with the higher values of LET and lower values for proton energy. MC calculations showed that LET_f value increased up to 5.2 keV/μm and 5.1 keV/μm, while LET_d value increased up to 6.5 keV/μm and 6.3 keV/μm for d_{WET} = 7.7 cm for PHITS and MCNP, respectively. For both MC codes, LET_d values were higher than LET_f values and relative difference of different LETs was up to 10% along the plateau and up to 25% in the BP. To enable comparison with the previously published studies, LET_w was also calculated using SRIM code (Ziegler et al., 2010). As shown in Fig 2.b, better agreement was obtained for LET_w and LET_f than for LET_w and $LET_{d.}$ Along the plateau (0.7 – 1.7 keV/μm) the relative difference between LET_w and LET_f was up to 2% and 5% for PHITS and MCNP respectively and it decreased up to 28% in the distal fall off region.

In this study, constant relative RPL efficiency, η_{RPL}, is observed along the plateau. LET_f values, calculated at the detector's positions in the plateau, ranged from 0.7 keV/μm to 1.7 keV/μm and an average value of the η_{RPL} (± standard deviation) was 1.00 ± 0.02. A 10% decrease of η_{RPL} is observed for the dosimeter within the BP with LET_f = 2.3 keV/μm. These results are in an agreement with the previous studies as will be discussed in the following.

There are not many data related to the RPL efficiency in the literature. Three studies were found that reported efficiency of RPL dosimeters type GD-302M as a function of LET in water (LET_w) for a clinical proton beam (Chang et al., 2017, Yasui et al., 2021, Nagata et al., 2021) and decrease of relative efficiency with the increase of LET was observed in all of them. Nagata et al. (2021) used scanning pencil proton beam and for the the LET_w range of (0.72 – 7.19) keV/μm decrease of relative efficiency from about 1.10 to 0.85 was observed. Very similar decrease was observed for passive scattered proton beams in the LET_w range of (1.63 – 8.13) keV/μm (Yasui et al., 2021). In the range from about 1 keV/μm to 3 keV/μm, a 10% decrease of relative efficiency was observed in all studies. In two other studies, RPL glasses were exposed to the high energy proton beams and a constant efficiency for LET_w of less than 0.5 keV/μm (Yasuda and Fujitaka, 2000) and 2 keV/μm (Kodaira et al., 2018) was reported. In both studies decrease of efficiency is observed when ion beams, having higher LET_w compared to proton beams used in the studies, were applied. In recent study (Majer et al., 2023), RPL glasses were exposed to the stopping, low energy proton beams and a steep decrease of efficiency is observed from 0.67 (for LET_w = 8.1 keV/μm) to 0.13 (for LET_w = 25.1 keV/μm).

A constant relative efficiency, η_{TLD}, for TLD-100 is observed for the investigated LET range, as well. For the investigated LET range, large changes were not expected. However, majority values are below unity and an average value of the η_{TLD} calculated for dosimeters positioned along the plateau (± standard deviation) is 0.97 ± 0.02. Although, there are many studies in the literature, the available experimental data for the relative TL efficiency of LiF:Mg,Ti dosimeters are not straightforward. In some studies, results indicate η_{TLD} which exceeds unity, while some studies reported η_{TLD} close or below unity (Avilla et al., 2006; Massillon et al., 2007; Sadel et al, 2015, Sadel et al, 2013, Sadel et al, 2016). However, the dosimeter preparation procedure as well as concentration of activators differs which could influence not only on supralinearity of dose response (Olko et al., 2001; Bilski et al., 1999), but also the relative efficiency may be changed as well. Other possible reasons that could affect the results are differences in the evaluation protocol used such as: different annealing conditions, heating rates, reference calibration and method of TL data evaluation. In general, for the LiF:Mg,Ti (type MTS-N) dosimeters, the η_{TLD} shows a maximum of about 1.10 – 1.15 for proton energy just above 20 MeV, what corresponds to LET_w = 2.5 keV/μm, while for lower and higher energies it decreases but stays over unity (Sadel et al., 2015). Results in this study are lower than unity and consistent with results published by Avilla et al. (2006) for TLD-100.

5. CONCLUSION

Dose dependence from 0.5 Gy to 9 Gy, and relative efficiency study was performed for RPL glass (type GD-302M) dosimeters and TLD-100 in the 100 MeV scanning pencil proton beam. RPLs showed linear dose response in the investigated dose range, while for TLDs supralinearity was observed. Same was confirmed in a ^{60}Co gamma ray field. A constant relative efficiency is observed along the plateau (corresponding to LET_f from 0.7 keV/μm to 1.7 keV/μm) of non-modulated proton beam with an average value 1.00 ± 0.02 for RPLs and 0.97 ± 0.02 for TLDs. A 10% decrease of relative efficiency is observed for RPL dosimeter within the Bragg peak with $LET_f = 2.3$ keV/μm. Relative difference of MCNP and PHITS MC code in calculating LET_f and LET_d was up to 5%. Future work will be focused on the evaluation of the efficiency for higher LET values using more energetic proton beams and precise positioning along the Bragg peak.

ACKNOWLEDGMENTS

This work was supported by the Croatian Science Foundation (Project IP-02-2020-3593).

The proton beam time has been provided in the frame of INSPIRE project (European Union's Horizon 2020 research and innovation programme under grant agreement no. 730983).

CONFLICT OF INTEREST

The authors have no conflict of interest to disclose.

REFERENCES

1. Araki, F., Ohno, T., 2014. The response of radiophotoluminescent glass dosimeter in megavoltage photon and electron beams. Med. Phys 41. https://doi.org/10.1118/1.4901639
2. Asgari, A., Ashoor, M., Sohrabpour, M. et al., 2015 Evaluation of various energy windows at different radionuclides for scatter and attenuation correction in nuclear medicine. Ann Nucl Med 29, 375–383. https://doi.org/10.1007/s12149-015-0950
3. ATGC, 2007. Explanation Material of RPL Glass Dosimeter: Small Element System. Tokyo, Japan: Asahi Techno Glass Corporation. https://www.c-technol.co.jp/eng/e-env_monitoring

4. Avila, O., Rodriguez.Villafuerte, M., Aviles, P., Gamboa-deBuen, I., Buenfil, A. E., Ruiz-Trejo, C., Concha, K., Brandan, M. E., 2006. TLD-100 thermoluminescent efficiencies for low-energy ions: correlation of efficiency with incident energy, J. Phys. D. Appl. Phys. 39, 2030-2037

5. Bilski, P., Olko, P., Burgkhardt, B., Piesch, E., Waligorski, M.P.R., 1994. Thermoluminescence Efficiency of LiF:Mg,Cu,P (MCP-N) Detectors to Photons, Beta-Electrons, Alpha Particles and Thermal Neutrons. Radiat Prot Dosimetry 55, 31–38. https://doi.org/10.1093/OXFORDJOURNALS.RPD.A082372

6. Bilski, P., Olko, P., Budzanowski, M., Ochab, E., Waligórski, M.P.R., 1999. Optimisation of LiF:Mg,Ti Detectors for Dosimetry in Proton Radiotherapy. Radiat. Prot. Dosim. 85, 367-372. https://doi.org/10.1118/1.3633892

7. Bilski, P., Budzanowski, M., Olko, P., Mandowska E., 2004. LiF:Mg,Ti (MTT) TL detectors optimised for high-LET radiation dosimetry, Radiat. Meas. 38, 427-430. https://doi.org/10.1016/j.radmeas.2003.12.013

8. Bilski, P., 2011. Calculation of the relative efficiency of thermoluminescent detectors to space radiation, Radiat. Meas. 46, 1728-1731. https://doi.org/10.1016/j.radmeas.2011.04.002

9. Boudard, A., Cugnon, J., David, J.-C., Leray, S., Mancusi, D., 2013. New potentialities of the Liège intranuclear cascade model for reactions induced by nucleons and light charged particles. Phys. Rev. C 87, 014606. https://doi.org/10.1103/PhysRevC.87.014606

10. Chang, W., Koba, Y., Katayose, T., Yasui, K., Omachi, C., Hariu, M., Saitoh, H., 2017. Correction of stopping power and LET quenching for radiophotoluminescent glass dosimetry in a therapeutic proton beam. Phys. Med. Biol. 62, 8869–8881. https://doi.org/10.1088/1361-6560/aa9155

11. Hirayama, H., Namito, Y., Bielajew, A. F., Wilderman, S. J., Nelson, W. R., 2005. The EGS5 code system. SLAC-R-730; KEK-REPORT-2005-8.

12. Horowitz, Y.S., Belaish, Y., Oster, L., 2006. Theories of TL systems: failures, successes, conflicts trends: insights into ossible future materials and techniques. Radiat. Prot. Dosim. 119, 124-129. https://doi.org/10.1093/rpd/nci695

13. Hsu, S.-H., Yang, H.-W., Yeh, T.-C., Hsu, W.-L., Wu, C.-H., Lu, C.-C., Chen, W.-L., Huang, D. Y. C., 2007. Synthesis and physical characteristics of radiophotoluminescent glass dosimeters, Radiat. Meas. 42, 621-624

14. Hsu., S.-M., Lee, J.-H., Hsu, F.-Y., Lee, H.-W., Hung, S.-K., Liao, Y.-J., Lee, M.-S., 2011. Dose measurements for gamma knife with radiophotoluminescent glass dosemeter and radiochromic film. Radiat. Prot. Dosim. 146, 256-259 https://doi.org/10.1093/rpd/ncr164

15. Iida, K., Kohama, A., Oyamatsu, K., 2007. Formula for Proton–Nucleus Reaction Cross Section at Intermediate Energies and Its Application. J. Phys. Soc. Japan 76, 044201. https://doi.org/10.1143/jpsj.76.044201

16. JCGM, 2008. Evaluation of measurement data-Guide to the expression of uncertainty in measurement. https://www.bipm.org/documents/20126/2071204/JCGM_100_2008_E.pdf/cb0ef43f-baa5-11cf-3f85-4dcd86f77bd6

17. Kalholm, F., Grzanka, L., Traneus, E., Bassler, N., 2021. A systematic review on the usage of averaged LET in radiation biology for particle therapy. Radiother. Oncol. 161, 211-221. https://doi.org/10.1016/j.radonc.2021.04.007

18. Kato, M., Chida, K., Moritake, T., Koguchi, Y., Sato, T., Oosaka, H., Tosa, T., Kadowaki, K., 2014 Fundamental study on the characteristics of a radiophotoluminescence glass dosemeter with no energy compensation filter for measuring patient entrance doses in cardiac interventional. Radiat. Prot. Dosim. 162, 224-229. https://doi.org/10.1093/rpd/nct300

19. Knežević, Ž., Beck, N., Milković, Đ., Miljanić, S., Ranogajec-Komor, M., 2011 Characterisation of RPL and TL Dosimetry System in Medical Dosimetry Applications, Radiat. Meas. 46, 201-1585. https://doi.org/10.1016/j.radmeas.2011.05.042

20. Knežević, Ž., Stolarczyk, L., Bessieres, I., Bordy, J. M., Miljanić, S., Olko, P., 2013. Photon Dosimetry Methods Outside the Target Volume in Radiation Therapy: Optically Stimulated Luminescence (OSL), Thermoluminescence (TL) and Radiophotoluminescence (RPL) Dosimetry, Radiat. Meas. 57, 9-18. https://doi.org/10.1016/j.radmeas.2013.03.004

21. Kodaira, S., Yanagida, Y., Koguchi, Y., Kawashima, H., Kitamura, H., Kurano, M., Ogura, K., 2018. Note: Complementary approach for radiation dosimetry with Ag+-activated phosphate glass. Review of Scientific Instruments 89, 116106. https://doi.org/10.1063/1.5058697

22. Majer, M., Pasariček, L., Knežević, Ž., Bokulić, T., Provatas, G., Božičević Mihalić, I., 2023. Relative efficiency of radiophotoluminescent glass detectors in low energy ion beams, Radiat. Meas. 166, https://doi.org/10.1016/j.radmeas.2023.106973

23. Massillon-JL, G., Gamboa-deBuen, I., Brandan, M. E., 2006. Onset of supralinear response in TLD-100 exposed to 60Co gamma rays, J. Phys. D.: Appl. Phys. 39

24. Massillon-JL, G., Gamboa-deBuen, I., Brandan, M. E., 2007. TL response of LiF:Mg, Ti exposed to intermediate energy 1H, 3He, 12C, 16O and 20Ne ions, J. Phys. D.: Appl. Phys. 40, 2584-2593

25. Miljanić, S., Ranogajec-Komor, M., Knežević, Ž., Vekić, B., 2002. Main Dosimetric Characteristic of Some Tissue-Equivalent TL Detectors, Radiat. Prot. Dosim. 100, 437-442. https://doi.org/10.1093/oxfordjournals.rpd.a005908

26. Miljanić, S., Ranogajec-Komor, M., Blagus, S., Pálfalvi, J.K., Pázmándi, T., Deme, S., Szántó, P., 2008. Response of radiophotoluminescent dosimeters to neutrons. Radiat. Meas. 43, 1068–1071. https://doi.org/10.1016/J.RADMEAS.2007.11.012

27. Nagata, J., Yasui, K., Omachi, C., Toshiyuki, T., Shimizu, H., Aoyama, T., Hayashi, N., 2021. Evaluation of radiophotoluminescent glass dosimeter response for therapeutic spot scanning proton beam: suggestion of linear energy transfer-based correction. J. Appl. Clin. Med. Phys. 22, 265–272. https://doi.org/10.1002/ACM2.13378

28. NIST, 2008., Table of X-ray Mass Attenuation Coefficients and Mass Energy-absorption Coefficients. National Institute of Standards and Technology. https://physics.nist.gov/PhysRefData/XrayMassCoef/tab4.html

29. Olko, P., Bliski, P., Budzanowski, M., Molokanov, A., Ochab, E., Waligorski, M. P. R., 2001. Supralinearity of peak 4 and 5 in thermoluminescent lithium fluoride MTS-N (LiF:Mg, Ti) detectors at different Mg and Ti concentration, Radiat. Meas. 33, 807-812. https://doi.org/10.1016/S1350-4487(01)00182-2

30. Olko, P., Bilski, P., 2020. Microdosimetric understanding of dose response and relative efficiency of thermoluminescence detectors, Radiat. Prot. Dosim. 192,165-177. https://doi.org/10.1093/rpd/ncaa211

31. Oonsiri, P., Kingkaew, S., Vannavijit, C., Suriyapee, S., 2019. Investigation of the dosimetric characteristics of radiophotoluminescent glass dosimeter for high-energy photon beams, J. Radiat. Res. and Apllied. Sciences. 12, 65-71. https://doi.org/10.1080/16878507.2019.1594092

32. Rah, J.-E., Hong, J.-Y., Kim, G.-Y., Kim, Y.-L., Shin, D.-O., Suh, T.-S., 2009. A comparison of the dosimetric characteristics of a glass rod dosimeter and thermoluminescent dosimeter for mailed dosimeter, Radiat. Meas. 44, 18-22. https://doi.org/10.1016/j.radmeas.2008.10.010

33. Rah, J. E., Oh, D.H., Shin, D., Kim, D.-H., Ji, Y.H., Kim, J.W., Park, S.Y., 2012. Dosimetric evaluation of a glass dosimeter for proton beam measurements. Applied Radiation and Isotopes 70, 1616–1623. https://doi.org/10.1016/J.APRADISO.2012.04.007

34. Sadel, M., Bliski, P., Swakon, J., Ptaszkiewicz, M., Boberek. M., Olko, P., 2013. Relative thermoluminescent efficiency of LiF detectors for proton radiation: Batch vaeiability and energy dependence. Radiat. Meas. 56, 205-208

35. Sadel, M., Bliski, P., Swakon, J., 2014. Relative TL and OSL efficiency to protons of various dosimetric materials. Radiat. Prot. Dos. 161, 112-115. https://doi.org/10.1093/rpd/nct217

36. Sadel, M, Bliski, P., Swakon, J., Rydygier, M., Howrwacik, T., Weber, A., 2015. Comparative investigation of the relative thermoluminescent efficiency of LIF detectors to protons at different proton therapy facilities, Radiat. Meas. 82, 8-13. https://doi.org/10.1016/j.radmeas.2015.07.009

37. Sadel, M., Bliski, P., Swakon, J., Weber, A., 2016. Evaluation of the relative efficiency of the thermoluminescent detectors to heavy charged particles, Radiat. Prot. Dosim. 168, 27-32. https://doi.org/10.1093/rpd/ncv003

38. Sato, T., Iwamoto, Y., Hashimoto, S., Ogawa, T., Furuta, T., Abe. S.-i., Kai, T., Tsai, P.-E., Matsuda, N., Iwase, H., Shigyo, N., Sihver, L., Niita, K., 2018. J. Nucl. Sci. Technol. 55, 684-690. https://doi.org/10.1080/00223131.2017.1419890

39. Son, K., Jung, H., Shin, S.-H., Lee, H.-H., Kim, M.-S., Ji, Y. H., Kim, K. B., 2011. Evaluation of the dosimetric characterisstics of a RPL glass dosimeters for high-energy photon and electron beams in the field of radiotherapy, Radiat. Meas. 46, 1117-1122. https://doi.org/10.1016/j.radmeas.2011.08.021

40. Stolarczyk, L., Trinkl, S., Romero-Expósito, M., Mojzeszek, N., Ambrozova, I., Domingo, C., Davidková, M., Farah, J., Kłodowska, M., Knežević, Liszka, M., Majer, M., Miljanić, S., Ploc, O., Schwarz, M., Harrison, R.M., Olko, P., 2018. Dose distribution of secondary radiation in a water phantom for a proton pencil beam—EURADOS WG9 intercomparison exercise. Phys. Med. Biol. 63, 085017. https://doi.org/10.1088/1361-6560/AAB469

41. Vekić, B., Ban, R., Miljanić, S., 2006. Second ary Standard Dosimetry Laboratory at the Ruđer Bošković Institute (in Croatian), Zagreb, Arh. Hig. Rada. Toksikol., 57, 189-194.

42. Wesolowska, P. E., Cole, A., Santos, T., Bokulić, T., Kazantsev, P., Izewska, J., 2017. Characterization of three solid state dosimetry systems for use in high energx photon dosimetry audits in radiotherapy, Radiat. Meas. 106, 556-562. https://doi.org/10.1016/j.radmeas.2017.04.017

43. Yamamoto, T., 2011. RPL Dosimetry: Principles and Applications. AIP Conf. Proc. 1345, 217. https://doi.org/10.1063/1.3576169

44. Yanagida, T., Okada, G., Kato, T., Nakauchi, D., Kawaguchi, N., 2022. A review and future of RPL dosimetry. Radiat. Meas. 158, 106847

45. Yasuda, H., Fujitaka, K., 2000. Responses of TLD-Mg2SiO4:Tb and Radiophotoluminescent Glass to Heavy Charged Particles and Space Radiation. Radiat. Prot. Dosim. 87, 115–119. https://doi.org/10.1093/OXFORDJOURNALS.RPD.A032983

46. Yasui, K., Omachi, C., Nagata, J., Toshito, T., Shimizu, H., Aoyama, T., Hayashi, N., 2021. Dosimetric response of a glass dosimeter in proton beams: LET-dependence and correction factor. Phys. Med. 81, 147–154. https://doi.org/10.1016/J.EJMP.2020.12.001

47. Ziegler, J.F., Ziegler, M.D., Biersack, J.P., 2010. SRIM – The stopping and range of ions in matter (2010) Nucl. Instrum. Methods Phys. Res. B. 268, 1818-1823. https://doi.org/10.1016/J.NIMB.2010.02.091

48. Yukihara, E. G., Doull, B. A., Ahmed, Md., Brons, S., Tessonnier T., Jakel, O., Greilich, S., 2015. Time-resolved opptically stimulated luminescence of Al2=3:C for ion beam therapy dosimetry, Phys. Med. Biol. 60, 6613

49. Werner CJ, Bull JS, Solomon CJ, Brown FB, McKinney GW, Rising ME, et al. 2018. MCNP version 6.2 Release notes. Report LA-UR-18-20808. Los Alamos Natl Lab